J. Min. Metall. Sect. B-Metall. 55 (2) B (2019) 261 - 270

Journal of Mining and Metallurgy, Section B: Metallurgy

SYNTHESIS OF DENDRITIC SILVER NANO POWDER USING PULSING ELECTROLYSIS IN AMMONIA SOLUTION

A. Soltanzadeh, S. Shahini, F. Rashchi*, M. Saba

University of Tehran, College of Engineering, School of Metallurgy and Materials Engineering, Tehran, Iran

(Received 14 June 2018; accepted 20 February 2019)

Abstract

A method to produce nano silver structures with high purity is pulsing electrolysis. In this paper the effects of potential, ammonia concentration (NH_3), silver ion concentration [Ag^+], total time, T_{on}, T_{off} and T_{rev} on this process were studied. The considered parameters were varied as follows: electrical potential = 5 – 10 V; [NH_3] = 40 – 80 g/L; [Ag^+] = 0.1 – 0.5 g/L; total time = 15 – 30 min; T_{on} = 1 – 8 ms; T_{off} = 1 – 8 ms; and T_{rev} = 0 – 4 ms. In order to optimize these parameters, the fractional factorial design of experiments was used. A silver dendritic structure was produced with nano size arm. The phase composition and morphology of the synthetized dendritic silver nanostructures was determined by X-ray diffraction (XRD) and scanning electron microscopy (SEM), respectively. The optimum condition to synthesize the dendritic silver nano powders were 7.52 V; [NH_3] = 64.75 g/L; [Ag^+] = 0.45 g/L; total time = 17.59 min; T_{on} = 6.97 ms; T_{off} = 4 ms; and T_{rev} = 1.89 ms. A mathematical model was also presented. The predicted silver nano size dendrite arm at the optimum condition was found to be 87.29 nm which was very close to the experimental value of 90 nm.

Keywords: *Pulsing electrolysis; Dendritic nanostructure; Ammonia medium; Nano silver*

1. Introduction

In recent years, nano structured metals have grown special attention due to their outstanding characteristics in comparison to their bulk form. Silver nano structure, especially, have privileged features such as significant electrical and thermal conductivity, germicidal action, and optical properties. These properties make silver nanostructures appropriate for electronics, medical, and chemical industries [1-3]. In solutions, by incorporating a capping agent, the surface molecules of nanostructures establish a double layer of charge that stabilizes particles independent of solution variables such as pH, and prevents aggregation due to repulsion of electrostatic forces. This feature makes dendritic silver structure a practical substance in surface chemistry applications. Silver nano structures present substantial light absorbing and scattering capabilities making them a suitable choice as a functional component in sensors and light devices [4, 5].

According to diversity and vast applications of nano structure materials, different methods have been utilized for production of nanostructured materials. These methods are categorized into three main divisions of chemical, physical, and mechanical-chemical. Atomization, electrodeposition, evaporation deposition, and mechanical commuting are examples of these methods. Among these methods, electrodeposition is remarkable due to its unique exclusivities such as highest purity, fine mechanical properties, ease of control, and low cost [6, 7].

Many researches have investigated deposition of dendritic silver nanostructure forming in different situations, methods and additives. In some researches dendritic silver structure has been synthesized using reduction agents such as sodium cyanide (NaCN) [8], sodium citrate ($C_6H_7NaO_7$) [9], sodium borohydride ($NaBH_4$) [10], and aniline ($C_6H_5NH_2$) [9, 11] in conventional nitrate media. The effect of additives like alkaline ions on the reduction process has also been studied in dendritic silver structure production [12].

Electrolysis by direct or pulsing current has been utilized to investigate nano silver production. In such researches organic additives such as poly vinyl pyrrolidone (PVP) with C_6H_9NO monomers or inorganic ones such as phosphate (PO_4^{3-}) have been utilized [13] directly performing a higher current

**Corresponding author: rashchi@ut.ac.ir*

DOI:10.2298/JMMB180614018S

efficiency and better physical appearance [14-17]. In some cases, additives have been used indirectly, only as contributory agent in the process as shape stabilizer or cluster controller [13, 14]. In recent researches, PVP has been used to decrease particle size. Also, PVP has been introduced as a stabilizer to increase the formation rate of particles [18, 19]. In a novel method, highly efficient and selective extraction of silver from electronic scrap has been achieved by means of dissolving the scrap in an ammonia medium activated by persulfate salt [20].

In some novel methods silver nano powder or mixed form of it with other metals has been synthesised by degradation of an organic compound [21]. Silver nanostructures have also been produced via sonochemical method. Dendritic silver nanostructure rods have been synthesised by ultrasonic irritation of the aqueous silver nitrate solution in presence of organic additives [22]. Pulsing electrolysis is a method to produce high purity nano powder that has been applied for producing nanosized copper powders [23]. It has been reported that by utilizing different regimes of electrolysis which are galvanostatic and potentiostatic, and by chemical route using hydrazine as reduction agent, various shapes and size distribution of silver powder have been obtained [24].

In direct current electrolysis, a negative charge layer surrounds the cathode, so that positive charge ions cannot reach the cathode. In pulsing mode, this layer is reduced during on-time current. Additionally, in reverse pulsing mode the whole layer disappears, and in sufficient reverse time a layer with opposite charge is formed resulting in a better ion migration to the cathode. Regions of electrolyte, especially around the cathode, will be deprived of metal ions during on-time electrolysis. In the rest time, ions migrate from more concentrated regions of the electrolyte to the less concentrated parts. Pulsing current increases limiting current by dramatic refilling metal ions in diffusion layer during the rest time. Moreover, utilizing high frequency pulsing current causes less additive consumption and reduces electrical conductivity of sediments [25].

In reverse pulsing electrolysis there are four independent variables, T_{on}, T_{off}, T_{rev} and peak current density. Considering these variables, desired chemical composition, porosity, and morphology can be controlled. In pulsing electrolysis, working cycle is defined as on-time out of total time ratio as defined below:

$$\gamma = \frac{T_{on}}{T_{on} + T_{off}} = Ton.f \tag{1}$$

where f is frequency and is defined as:

$$f = \frac{1}{T_{on} + T_{off}} \tag{2}$$

If in the working cycle there is a reverse time:

$$\gamma = \frac{T_c}{T_{AA} + T_C} \tag{3}$$

where T_c is the cathodic reverse time and T_{AA} is the anodic reverse time.

In practice, pulsing electrodeposition includes a 5% working cycle or more and on-time varies from μs to ms. Metal deposition rates in both forms are equal if average current density (I_A) in pulsing electrodeposition corresponds to current density in direct current form which is defined below:

$$I_A = Peak\ current\ density\left(I_P\right) \times working\ cycle\left(\gamma\right) \tag{4}$$

and in a reverse time:

$$I_A = \frac{I_c T_c - I_{AA} T_{AA}}{T_{AA} + T_c} \tag{5}$$

where I_{AA} is anodic current density and I_c is cathodic current density [25, 26].

Electrochemical deposition consists of two main stages of nucleation and growth. Increase in the nucleation rate results in the formation of more nuclei sites, thus the mean size of structures and particles is reduced [27]. One of the advantages of pulsing electrolysis in comparison to direct current electrolysis is the increase in nucleation rate and the decrease in growth rate. Size reduction is the main outcome of this phenomenon [28].

In this research, dendritic silver nanostructure has been fabricated in ammonia solution by means of pulsing electrolysis and its characteristics have been systematically investigated. The effect of potential, ammonia concentration (conc.), silver ion concentration, total electrolysis time and pulsing time factors (T_{on}, T_{off} and T_{rev}) were studied on nanostructure dendrite arm size (DAS) and related morphologies. The design of the experiment was applied through the process to obtain a suitable mathematical model and optimized experimental factors in terms of the structure size.

2. Experiments

2.1. Materials

The cathode was made of stainless steel, and a graphite anode was selected. Ammonia, silver chloride (99.9%), and acetone (CH_3COCH_3) were all purchased from Merck, Germany and used as received and without further purification. Deionized water was used in the experiments.

2.2. Synthesis

2.2.1. Preparation

A piece of stainless steel cathode (25×40 mm) and a graphite anode were used. The cathode and the anode were sealed with varnish to attain the desired area. The surface of the cathode was cleaned by abrasive paper (SIC sand paper) with 120, 240, 400, 600 and 1200 mesh sizes. Then, the anode and the cathode were immersed in a beaker filled with acetone in ultrasonic bath device for 10 min (BANDELIN sonorex, 130 W) to degrease organic contaminations, especially fatty acids. Then, both were washed with deionized water several times. Both the cathode and the anode were dipped into a glass reactor (a 100 mL beaker) filled with electrolyte in parallel situation facing each other with a constant distance of 5 cm.

2.2.2. Powder preparation

A rectifier (SL20RPC-IPC, Iran) was used to deposit the powder. The electrolyte was a mixture of ammonia, silver chloride and deionized water. Average current density was 0.05 A/cm^2. The experiments were performed in a 100 mL beaker equipped with a magnetic stirrer (IKA RH Basic2 from Germany). Cathodic current density was selected twice as much as anodic current density as suggested by Naboychenko and Murashova, 2009. The anode and the cathode were sealed with varnish to obtain the mentioned ratio. The deposited silver powder was brushed from the cathode surface mechanically and the cathode was washed with deionized water. Then, the powders were submerged immediately into acetone to prevent subsequent oxidation. The powders were dispersed via magnetic stirring for about 20 min followed by 40 min ultra-sonication in an ultrasonic bath (VGT-1730QTD, Korea) at pH ca. 9.5 to prevent formation of agglomerates. The temperature was kept constant at 25 °C and the solution was in good-mixing condition through magnetic stirring [29].

2.3. Characterization

Phase composition of the dried powders was tested by X-ray diffraction (XRD, X'pert Philips) which is shown in Figure 1. According to the results the silver powder is pure. Scanning electron microscopy (SEM, CamScan MV2300) was utilized to investigate the powder morphology. Average particle size was determined by a laser particle size analyzer (LPAS, Cilas 1061).

2.4. Design of experiments (DOE)

Variable parameters and their ranges are given in

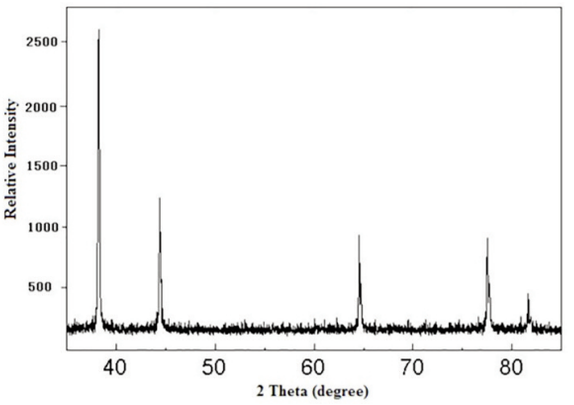

Figure 1. *XRD pattern of silver nano powders*

Table 1. Experiment results and modeling predictions are shown in Table 2. All statistical studies were accomplished on particle sizes and the main investigation aim was to achieve minimum size. A fractional factorial design was developed for this purpose. Factors were studied in two levels of high or low limits. To perform factorial design, measurement units that represent experimental factors were coded into -1 as low and +1 as high limitations. The design response indicates nano silver dendrite arm size (DAS). A fractional factorial design is presented by $2^{(k-p)}$ formula, where k is number of factors and $1/2^p$ is fraction of full factorial. By this order, an experiment would be performed at two levels with k factors in just $2^{(k-1)}$ while a full factorial design demands 2^k distinct experiments. The DESIGN EXPERT 8.0.1 trial version (State-Ease Inc., Minneapolis, MN, USA) software was utilized to data regression and graphical analysis development. In this article 7 parameters were studied at two levels using a $1/2^4$ fraction factorial. Thus, $2^{(7-4)}$= 8 runs were required to establish a satisfactory design [30].

Table 1. *Variable parameters, range values and codification of the factors*

Factor	Name	Units	Coded	
			-1	1
A	Potential	V	5	10
B	Ammonia Conc.	g/L	40	80
C	AgCl Conc.	g/L	0.1	0.5
D	Total time	min	15	30
E	T_{on}	ms	1	8
F	T_{off}	ms	1	8
G	T_{rev}	ms	0	4

Table 2. *Experiment results and model predictions*

Experiment number	A	B	C	D	E	F	G	Ag size (nm)	
								Actual	Predicted
1	5	40	0.1	30	8	8	0	159	150
2	10	40	0.1	15	1	8	4	ND*	
3	5	80	0.1	15	8	1	4	135	112.5
4	10	80	0.1	30	1	1	0	600	370
5	5	40	0.5	30	1	1	4	ND	
6	10	40	0.5	15	8	1	0	142	150
7	5	80	0.5	15	1	8	0	140	370
8	10	80	0.5	30	8	8	4	90	112

3. Results and discussion

3.1. Metallurgical

3.1.1. Mechanism

During the electrodeposition of silver in ammonia solution under the applied potential, the following reactions occur [31]:

The cathodic reactions are:

$$Ag\left(NH_3\right)_2^+ + e^- = Ag + NH_3 \quad E^\circ = +0.373V \tag{6}$$

$$2H_2O + 2e^- = H_2 + 2OH^- \quad E^\circ = -0.829V \tag{7}$$

The anodic reaction is:

$$4OH^- = O_2 + 2H_2O + 4e^- \quad E^\circ = +0.401V \tag{8}$$

The standard silver reduction reaction is:

$$Ag^+ + e^- = Ag \quad E^\circ = +0.799V \tag{9}$$

which is replaced by reaction (6) in ammonia solution. Silver ions form a stable complex in ammonia solution $[Ag\left(NH_3\right)_2^+]$, consequently, the standard reduction potential changes.

Reaction (7) shows a possible reduction reaction that is able to compete with the silver ions/species during electrowinning at high pHs. However, the difference between the standard reduction potential of reactions (6) and (7) is high enough to avoid the reduction of water and the formation of hydrogen gas (H_2) over the cathode. The silver complex species possess a higher tendency to be reduced in comparison to water decomposition reaction, thus it overcomes the water reduction reaction.

During the process, bubbles were observed around the graphite anode. Also, there was no other chemical component in the solution to be oxidized, except the hydroxide ions. Thus, the oxidation of the hydroxide ions is the only possible oxidation reaction that can occur in the anode. Therefore, reaction (8) is the proper anodic oxidation reaction. The bubbles seen around the anode are oxygen bubbles (O_2) generated due to reaction (8) [31-33].

Ammonia solution has three key advantages. Firstly, corrosion rate in this medium is less than in acidic medium. Therefore, maintenance expenses are lower than in the acidic media and material durability is higher in comparison to the acidic ones, which makes this medium more economical. Secondly, according to the reactions (6) and (7) and the high standard potential differences, there is no hydrogen gas emission, resulting in more silver powder adhesion to the cathode. Moreover, the produced powder will not be dispersed in the solution. Additionally, the absence of hydrogen ions (H^+) in reduction half-equation prevents hydrogen over potential in the cathode, which causes a better reduction efficiency. Another reason for choosing ammonia solution is hydrometallurgical issues for silver. The ammonia solution is one of the best media for the selective extraction of silver ions from other metallic ions. Silver ions form a stable complex in ammonia solution. The stability of ammonia-based complexes is temperature dependent, therefore, in co-extraction of various metallic ions, it is possible to separate and precipitate undesired ions by temperature control [31, 32, 34].

3.1.2. Silver ion (Ag^+) concentration

The silver ion concentration has a mild effect on the electrolysis process. This is due to the fact that during electrolysis, a diffusion layer (Nernst layer) controls ions migration onto the cathode surface. Thus, a steady gradient of concentration is formed during on-time, which results in a constant reduction rate under this condition. During reverse and off-time, the thickness of Nernst layer becomes thinner; however, the bigger on-time magnitude and high frequency in a working cycle and lack of agitation keep this layer stable. Therefore, the presence of ions and their concentration are independent of total Ag concentration and is related to the diffusion in Nernst layer [31].

3.1.3. Ammonia concentration

As mentioned before, silver ions tend to form a stable complex with ammonia. This complex called diamine silver (I) makes silver less susceptible to reduction. Related reduction reactions are reaction (9) and the one presented below:

$$3Ag\left(NH_3\right)_2^+ + 3OH^- = 3Ag + 5NH_3 + 3H_2O + 0.5N_2 \qquad E^0 = +0.373\ V \tag{10}$$

Reaction (10) shows the formation and decomposition of silver complexes in ammonia media. According to the standard potentials, the silver complex is more difficult to be reduced than the single silver ions. On the other hand, as the ammonia

concentration increases, more silver ions turn into the ammonia complex, and the reduction tendency is decreased. This fact results in a finer structure of silver [34, 35].

3.1.4. Total time

During electrolysis, several working cycles including on, off, and reverse time occur. As illustrated before, Nernst layer thickness alternatively changes during the cycles and the three main parameters of these cycles mainly affect this layer and the nucleation and growth processes. Total time only determines the number of cycles, whereas cycle type and its parameters are important factors, not the numbers [23].

3.1.5. Potential

Voltage directly influences the peak current density. Thus, increment in voltage increases the current density. In high current density, reduced ions find no opportunity to accommodate in the proper sites of a metal crystal lattice. A finer structure takes place while the nucleation rate exceeds the nuclei growth rate. The nucleation rate as a function of external voltage is defined as:

$$\upsilon = K_1 \exp\left(\frac{-K_2}{V}\right) \quad (11)$$

where K_1 and K_2 are constants and υ is the applied over voltage.

According to formula (10), as the applied over voltage increases (as well as the external potential) the nucleation rate increases leading to more nucleation sites rather than nuclei growth, resulting in a finer structure [23, 36].

3.1.6. T_{off} (off-time)

T_{off} is defined as the time when current density is cut off, and during this time no potential is applied to the whole system. The effect of off-time is in Nernst layer reduction, ion agitation, and reposition around the cathode. But during off-time no current is applied; thus, the mentioned alternations are time consuming. Since high frequency and duration off-time in each working cycle is low, this factor shows little effect in the data analysis [23, 37].

3.1.7. T_{on} and T_{rev}

One of the important factors in structure size determination is the nucleation process. Nucleation is related to the reduction rate of metallic ions on the cathode surface that determines the number of nuclei, or in other words - nucleation rate. As the nucleation rate is increased, the local reduction sites on the cathode surface are grown up. More reduction sites bring about more growing nuclei in a constant reduction area. At last, these growing nuclei construct the final structure which is finer due to the more nuclei constituting it.

In an average current density, the ion reduction process and the created nucleus sites are time dependent phenomena. In other words, when there is an established current, the only determining factor in the number of nuclei is the reduction time. T_{on} is the time whenthe current direction is analogous to direct electrolysis and causes the stainless steel specimen to become the cathode (the cathode is the negative terminal, from which current exits the device and returns to the external generator). During T_{on}, ions have opportunity to be reduced on a cluster of former reduced ions or create a new nucleus. In contrast, $T_{reverse}$ or T_{rev} is the time when current direction is opposite in respect to T_{on}, which results in an opposite charge on the cathode surface. In other words, during T_{off} negative terminal turns to a positive one. An effect of this phenomenon is the re-oxidation of the reduced ions. Thus, former reduction sites (nuclei) oxidize into ions and the number of these sites is decreased.

According to what has been explained earlier, increasing T_{on} metallic ions provides more opportunities to construct new reduction sites, (nuclei) leading to a finer structure. By decreasing T_{on}, ions have less time to construct new reduction sites. These ions are reduced on a cluster of former reduced ions which has a lower energy barrier. In comparison, by increasing in T_{off}, the newly formed nuclei will be oxidized into ions, and the number of nuclei decreases. This phenomenon leads to a coarser structure [23, 25, 38].

3.2. Morphology analysis

The SEM micrographs of a typical series of silver nano structured samples obtained from experiments are shown in Figures 2 and 3. The most noticeable feature of these images is their similar morphology. All of the samples have dendritic structures with nano sized arm structure which is called dendritic nano structure concisely [39].

Figure 2a shows SEM micrograph of the experiment number 1, indicating an average dendrite arm size of 159 nm. Figure 2b shows an average size of 135 nm for the dendrite arm regarding the experiment number 3 powders. The results of the experiment number 6, Figure 2c, show 142 nm for dendrite arm size. Figure 2d, experiment number 8, shows the finest structure among others. According to the software calculations, the average dendrite arm size in this sample is 90 nm.

Briefly, all the particle sizes are in the range of 90

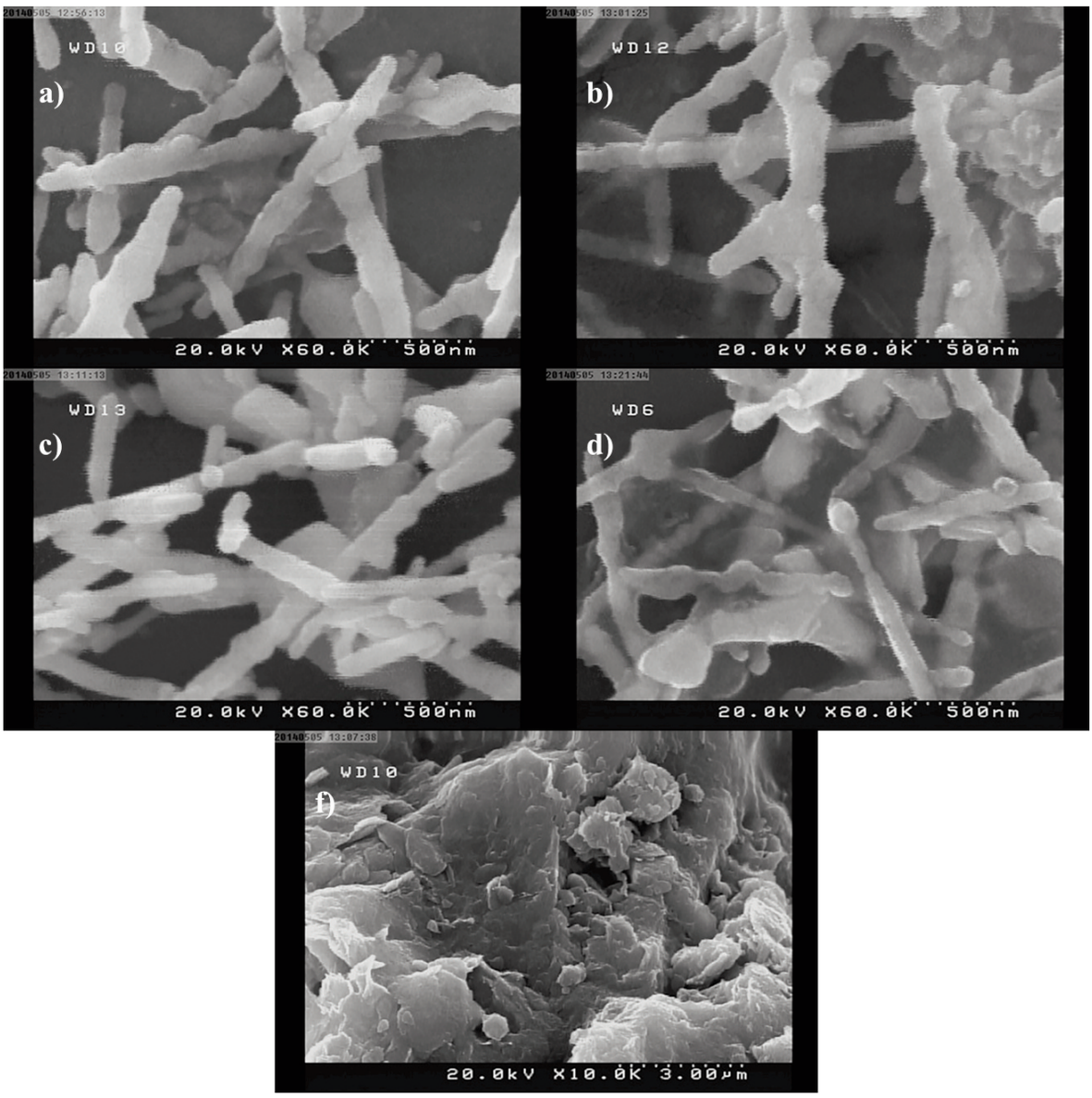

Figure 2. *(a - f) – SEM micrograph of dendritic silver nano powders obtained from experiment (a) No. 1, (b) No. 3, (c) No. 6, (d) No. 8, (f) No. 4*

nm to 159 nm. Figure 2f shows SEM micrograph of silver nano powders obtained from experiment No. 4. In Figure 2f, the morphology and the average size of the dendritic arm alter dramatically. The significant drop in T_{on} has a direct effect on the size reduction. Furthermore, it can be concluded that the reduction in T_{on} will influence the morphology directly, and this reduction can cause principal alternation even from a dendritic silver nanostructure type to a bulk one.

SEM micrograph of silver nano powders obtained from experiment No. 7 is shown in Figure 3a and 3b. As can be seen from Figure 3a and b, despite the fact that T_{off} has a slight effect on the average size according to the previous section and statistical analysis which will be discussed later, this experimental factor can play a considerable role in the evolution of the morphology. In this sample both spherical (Figure 3a) and dendritic (Figure 3b) structures are observable. With further scrutiny, dendritic tendency to spherical form is also obvious (Figure 3b). Another considerable point is the particle size in the spherical type. Although higher T_{off} can change the morphology, it cannot influence the average size. The average particle size is out of the nano range due to the low T_{on}.

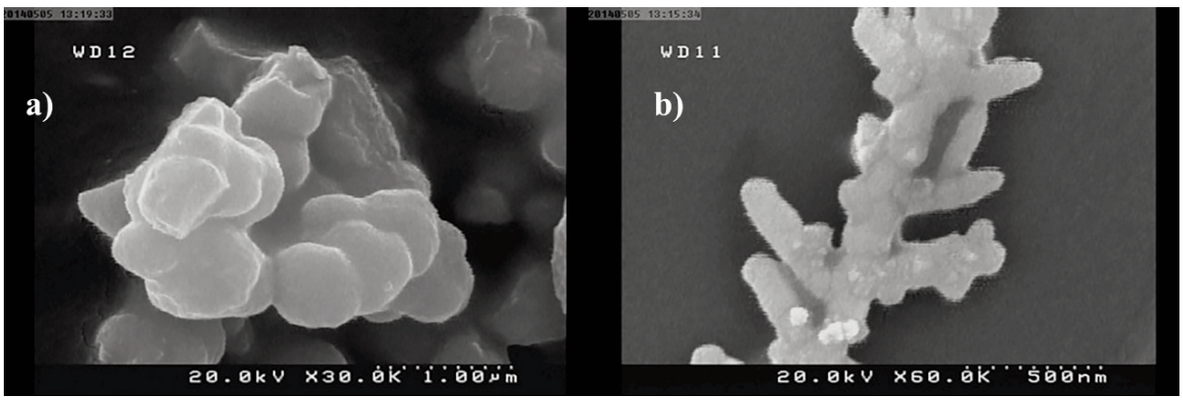

Figure 3. *(a and b) – SEM micrographs of silver nano powders obtained from experiment No. 7, (a) spherical, (b) dendritic*

3.3. Analysis of variance (ANOVA)

Table 3 shows the results of the ANOVA test performed by the DX8 software. None of the parameters have p-values less than 0.05, indicating that they are significant at a 95.0% confidence level. Moreover, the pareto chart (Figure 4) indicates that the most important parameters on the dendrite arm size of silver nanostructures are the effects of the individual factors of T_{on} (E), ammonia concentration (B) and T_{rev} (G), respectively. From a statistical perspective, Figure 5a illustrates the effect of T_{on} on dendrite arm size of silver nanostructures (DAS). This figure implicitly shows that increment in T_{on} results in finer structures, which is a verification for the metallurgical explanation discussed previously in section 3.1. Figures 5a and b exhibit a similar concept. Figure 5b illustrates the effect of ammonia concentration on DAS proposing an indirect effect on the structure size meaning DAS and ammonia concentration have inverse reciprocal relation. Figure 6 shows the effect of T_{rev} on DAS. By increasing T_{rev}, DAS will be coarser. According to Table 3, for silver dendrite arm size, the "F-value" of <0.0001 (as measured by difference between the average of the center points and the average of the factorial points) implies that the curvature in the design space is not significant relative to the noise.

Table 3 shows the coefficients of the variables in the model. Empirical relationships between the responses and the variables can be expressed by the following fitting model:

$$R(nm) = +10759.92857 - 120.85\,ammonia\,conc. - 721.92857\,T_{on} + 1199\,T_{rev} \quad (12)$$

where R is DAS.

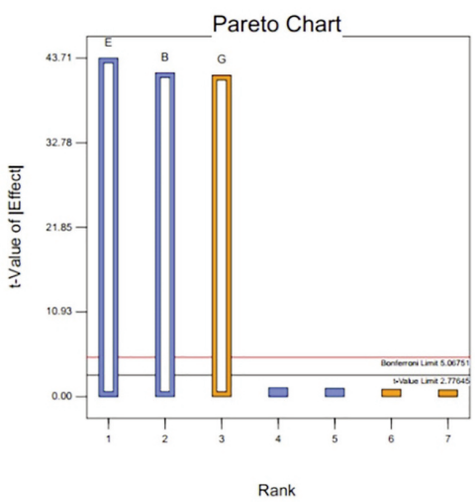

Figure 4. *Pareto chart of independent variables*

Table 3. *Analysis of variance*

Source	Sum of Squares	DF	Mean Square	F Value	p-value Prob>F	
For Silver nano DAS						
Model	1.438E+008	3	4.794E+007	1792.80	<0.0001	significant
B-Ammonia Conc.	4.674E+007	1	4.674E+007	1747.81	<0.0001	
E-T_{on}	5.108E+007	1	5.108E+007	1910.14	<0.0001	
G-T_{rev}	4.600E+007	1	4.600E+007	1720.44	<0.0001	
Residual	1.070E+005	4	26739.25			
Cor Total	1.439E+008	7				

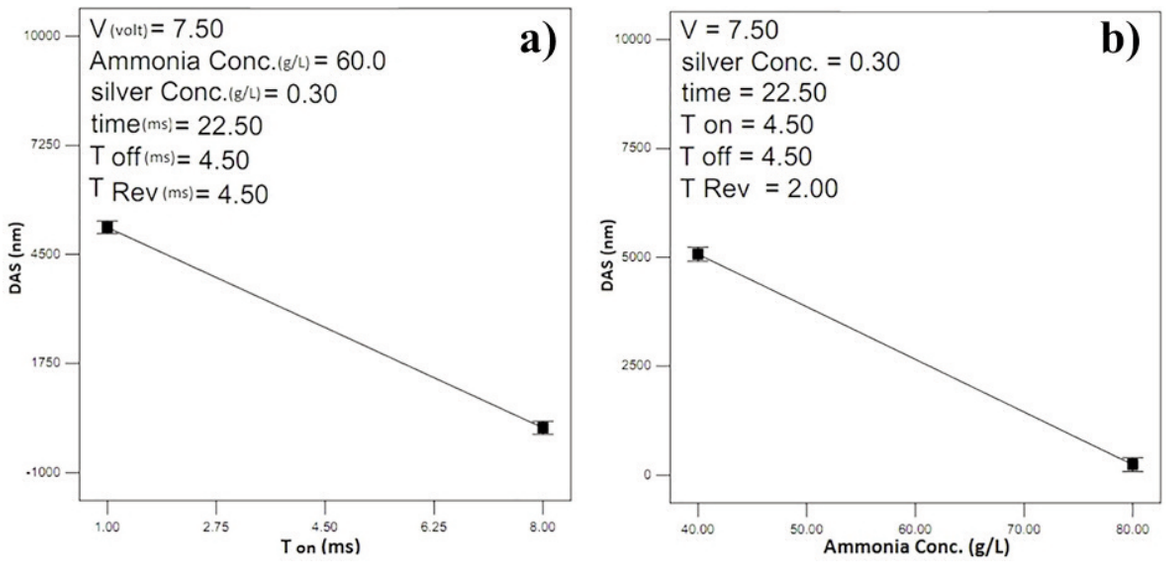

Figure 5. *(a –b) – Effect of (a) Ton and (b) ammonia concentrate on silver nano dendrite arm size*

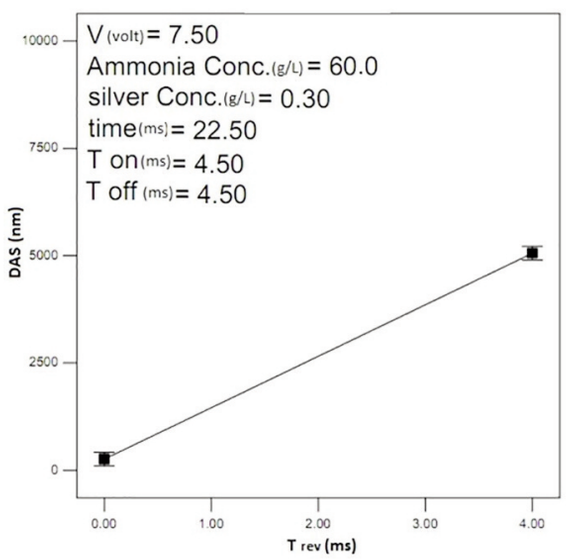

Figure 6. *Effect of T_{rev} on silver nano dendrite arm size*

The model developed in this study predicts the dendrite arm size of silver nanostructures from an ammonia silver solution. Joglekar and May (1987) stated that for a proper fit to the model, the correlation coefficient should be at least 0.80. In the present case, the correlation coefficient was higher than 0.80 ($R^2_{(DAS)}$ = 0.99), indicating that there is a good agreement between the model and experimental values. The "Model F-value" of 1792.80 implies that the model is significant. There is only a 0.01% chance that a "Model F-Value" this large could occur due to noise. In this case E, B, G are significant model terms. Presented data in Table 3 show a good agreement between the model and experimental results at 95% confidence level for silver nano dendrite arm size. Finally, by using the parameters of the obtained model, the optimized condition for silver nano DAS is (potential of 7.52 V, ammonia concentration of 64.75 g/L, Ag^+ of 0.45 g/L, total time of 17.59 min, T_{on} of 6.97 ms and T_{off} of 4 ms and T_{rev} of 1.89 ms) that results in dendritic silver nanostructure DAS of 87.29 nm.

4. Confirmation test

Confirmation tests were repeated three times with the actual dendritic silver nanostructure DAS of 90.62 nm, 91.01 nm and 88.84 nm which had less than 5% deviation from calculated maximum silver nano DAS (87.29 nm) predicted by the model.

5. Conclusions

1) The effects of seven parameters have been investigated on dendritic silver nano powder and dendritic silver morphology: potential, 5–10 V; [NH_3], 40–80 g/L; [Ag^+], 0.1–0.5 g/L; total time, 15–30 min; T_{on}, 1–8 ms; T_{off}, 1–8 ms; and T_{rev}, 0–4 ms. Among these, three parameters including T_{on}, ammonia concentration [NH_3] and T_{rev} have the major influence on dendrite arm size.

2) The produced powder has a dendritic structure with nano size dendrite arm size. DAS in different experimental conditions varies from 90 nm to 159 nm. Morphology alternation has been obtained.

3) A fractional factorial design was utilized to create a mathematical model in order to optimize major experimental factors. The model is shown in following equation:

R(nm) = +10759.92857-120.85 ammonia conc.-721.92857 T_{on}+1199 T_{rev}

4) Three confirmation tests proved the optimum condition (potential of 7.52 V, ammonia conc. 64.75 g/L, Ag^+ of 0.45 g/L, total time of 17.59 min, T_{on} of 6.97 ms and T_{off} of 4 ms and T_{rev} of 1.89 ms). These tests determined DAS suggested by optimized model (87.2 nm) with less than 5% deviation.

References

[1] L. Rizzello, R. Cingolani, P.P. Pompa, Nanomedicine., 8(5) (2013) 807-821.

[2] K. Vahabi, S.K. Dorcheh, Biotechnology and biology of trichoderma, Elsevier, Waltham, 2014, p.393-404.

[3] M. Rashidi Huyeh, M. Shirdel Havar, B. Palpant, J. Appl. Phys., 112(10) (2012) 103-101.

[4] P.I. Gaiduk, J. Chevallier, S.L. Prokopyev, A. Nylandsted Larsen, Microelectron. Eng., 125 (2014) 68-72.

[5] M. Badawy, P. Luxton, G. Silva, G. Scheckel, T. Suidan, M. Tolaymat, Environ. Sci. Technol, 44(4) (2010) 1260-1266.

[6] W.L. Peter, A.I.H. Committee, ASM Handbook: Volume 7: Powder Metal Technologies and Applications (E. Klar), ASM International, Geauga County, 1998.

[7] W. Liu, S. Hsieh, W. Chen, P. Wei, J. Lee, Int. J. Min. Met. Mater., 16(1) (2009) 101-107.

[8] S.K. Ghosh, S. Kundu, M. Mandal, S. Nath, T. Pal, J. Nanopart. Res., 5(5-6) (2003) 577-587.

[9] Z. Khan, S.A. Al-Thabaiti, A.Y. Obaid, A.O. Al-Youbi, Colloid. Surface. B., 82(2) (2011) 513-517.

[10] Y.A. Krutyakov, A.A. Kudriniskiy, A.Y. Olenin, G.V. Lisichkin, Rus. Chem. Rev., 77(3) (2008) 233-257.

[11] Y. Tan, Y. Li, D. Zhu, J. Colloid. Interf. Sci., 258(2) (2003) 244-251.

[12] K.S. Chou, Y.C. Lu, H.H. Lee, Mate. Chem. Phys., 94(2-3) (2005) 429-433.

[13] L. Rodriguez-Sanchez, M. Blanco, M. Lopez-Quintela, J. Phys. Chem. B., 104(41) (2000) 9683-9688.

[14] H. Ma, B. Yin, S. Wang, Y. Jiao, W. Pan, S. Huang, S. Chen, F. Meng, Chem. Phys. Chem, 5(1) (2004) 68-75.

[15] M.T. Mendez-Aguilar, F.J. Garfias-Ayala, F.J. Garfias-Vazquez, ECS. Transactions., 36(1) (2011) 283-290.

[16] G. Zarkadas, A. Stergiou, G. Papanastasiou, J. Appl. Electrochem., 34(6) (2004) 607-615.

[17] K.I. Popov, M.G. Pavlovic, B.N. Grgur, J. Appl. Electrochem., 28(8) (1998) 797-801.

[18] V. Sáez, T.J. Mason, Molecules., 14(10) (2009) 4284-4299.

[19] I. S. Haas, S. Shanmugam, A. Gedanken, J. Phys. Chem. B., 110(34) (2006) 16947-16952.

[20] W. Hyk, K. Kitka, Waste. Manage., 60 (2017) 601-608.

[21] P. Khanna, B. Das, Mater. Lett., 58(6) (2004) 1030-1034.

[22] Y.P. Zhu, X.k. Wang, W.L. Guo, J.G. Wang, C. Wang, Ultrason. Sonochem., 17(4) (2010) 675-679.

[23] R.K. Nekouei, F. Rashchi, A. Ravanbakhsh, Powder. Technol., 250 (2013) 91-96.

[24] L. Avramović, M. Bugarin D. Milanović, V. Conić, M.M. Pavlović, M. Vuković, N.D. Nikolić, J. Min. Metall. Sect. B: Metall., 54(3) B (2018) 291-300.

[25] M. Chandrasekar, M. Pushpavanam, Electrochim. Acta., 53(8) (2008) 3313-3322.

[26] N. Mandich, Met. Finish., 97(1) (1999) 375-380.

[27] J. Xue, Q. Wu, Z. Wang, S. Yi, Hydrometallurgy., 82(3-4) (2006) 154-156.

[28] M. Tesakova, V. Parfenyuk, Surf. Eng. Appl. Elect., 46(5) (2010) 400-405.

[29] X. Li, D. Zhu, X. Wang, J. Colloid. Interf. Sci., 310(2) (2007) 456-463.

[30] R.K. Nekouei, F. Rashchi, A.A. Amadeh, Powder. Technol., 237 (2013) 165-171.

[31] M.G. Fontana, Corrosion engineering, McGraw-Hill, New York, 1987.

[32] R.W. Revie, H.H. Uhlig, Corrosion and corrosion control, John Wiley & Sons INC., Hoboken, 2008.

[33] S. Viswanath, G. Sajimol, Metalurgija., 17(2) (2011) 57-69.

[34] B.Z. Shakhashiri, Chemical demonstrations: A handbook for teachers of chemistry. Vol. 2, University of Wisconsin Press, Madison, 1985.

[35] J. Dentzer, P. Ehrburger, J. Lahaye, J. Colloid. Interf. Sci., 112(1) (1986) 170-177.

[36] W. He, X.C. Duan, L. Zhu, J. Cent. South. Univ. T., 16(5) (2009) 708.

[37] N. Ibl, Surf. Technol., 10(2) (1980) 81-104.

[38] D. Landolt, A. Marlot, Surf. Coat. Tech., 169 (2003) 8-13.

[39] H.P. Ding, G.Q. Xin, K.C. Chen, M. Zhang, J. Hao, H.G. Liu, Colloid. Surface. A., 353(2-3) (2010) 166-171.

SINTEZA DENDRITNOG NANO PRAHA SREBRA KORIŠĆENJEM PULSIRAJUĆE ELEKTROLIZE U RASTVORU AMONIJAKA

A. Soltanzadeh, S. Shahini, F. Rashchi*, M. Saba

Univerzitet u Teheranu, Fakultet za inženjerstvo, Odsek za metalurgiju i inženjerstvo materijala, Teheran, Iran

Apstrakt

Pulsirajuća elektroliza je metod za proizvodnju nanostruktura srebra velike čistoće. U ovom radu su proučavani efekti potencijala, koncentracije amonijaka (NH_3), koncentracije jona srebra [Ag^+], i ukupnog vremena, T_{on}, T_{off} i T_{rev}. Razmatrani parametri su menjani na sledeći način: električni potencijal = 5 – 10 V; [NH_3] = 40 – 80 g/L; [Ag^+] = 0.1 – 0.5 g/L; ukupno vreme = 15 – 30 min; T_{on} = 1 – 8 ms; T_{off} = 1 – 8 ms; i T_{rev} = 0 – 4 ms. Da bi se ovi parametri optimizirali korišćen je frakcionalni faktorijalni eksperimentalni dizajn. Dobijena je dendritna struktura srebra sa granom nano veličine. Fazna kompozicija i morfologija tako sintetizovanih dendritna nanostruktura srebra određena je rendgenskom defrakcijom (XRD) i elektronskim skenirajućim mikroskopom (SEM). Optimalni uslovi za sintetizovanje dendritičkih nano prahova srebra bili su 7.52 V; [NH_3] = 64.75 g/L; [Ag^+] = 0.45 g/L; ukupno vreme = 17.59 min; T_{on} = 6.97 ms; T_{off} = 4 ms; i T_{rev} = 1.89 ms. Takođe je predstavljen i matematički model. Predviđena dendritna grana srebra nano veličine bila je 87.29 nm, što je veoma blizu eksperimentalne vrednosti od 90 nm.

Ključne reči: *Pulsirajuća elektroliza; Dendritna nanostruktura; Rastvor amonijaka; Nano srebro*